The Journal of Immunology

Hyaluronan Induces Cell Death in Activated T Cells through CD44

Brian Ruffell and Pauline Johnson

J Immunol 2008; 181:7044-7054; ;
doi: 10.4049/jimmunol.181.10.7044
http://www.jimmunol.org/content/181/10/7044

The Journal of Immunology is published twice each month by
The American Association of Immunologists, Inc.,
1451 Rockville Pike, Suite 650, Rockville, MD 20852

Print ISSN: 0022-1767 Online ISSN: 1550-6606.

Hyaluronan Induces Cell Death in Activated T Cells through CD44[1]

Brian Ruffell and Pauline Johnson[2]

In the immune system, leukocyte activation induces CD44 to bind hyaluronan, a component of the extracellular matrix. Here we used gain and loss of hyaluronan-binding mutants of CD44 to examine the consequence of hyaluronan binding in T cells. Jurkat T cells transfected with CD44 mutated at S180, which prevented the addition of chondroitin sulfate, displayed constitutively high levels of hyaluronan binding. These cells were more susceptible to activation-induced cell death, whereas cells expressing a CD44 mutant unable to bind hyaluronan (R41A) were resistant to cell death. In TCR or PMA activated Jurkat T cells, hyaluronan induced rapid cell death. This depended on the level of hyaluronan binding by the cell, and the amount and size of hyaluronan. High molecular mass hyaluronan had the greatest effect and cell death occurred independently of Fas and caspase activation. In splenic T cells, high hyaluronan binding occurred in a subpopulation of cells undergoing activation-induced cell death. In addition, hyaluronan induced cell death in ~10% of reactivated splenic T cells when Fas-dependent apoptosis was prevented by Ab blocking or in Fas negative MRL/*lpr* T cells. This demonstrates that hyaluronan can induce cell death in activated, high hyaluronan binding T cells via a Fas-independent mechanism. ***The Journal of Immunology,*** **2008, 181: 7044–7054.**

CD44 and its ligand hyaluronan (HA)[3], an extracellular matrix glycosaminoglycan, have been implicated in a number of processes including wound healing, inflammation, angiogenesis, and metastasis (reviewed in Refs. 1–6). In immune-mediated diseases, CD44 can either augment or reduce symptoms. For example, $CD44^{-/-}$ mice have reduced disease severity in autoimmune models of atherosclerosis (7) and arthritis (8), whereas disease severity is increased in mouse models of lung inflammation (9) and inflammatory bone loss (10). In T cells, the evidence suggests a largely proinflammatory role for CD44. Increased expression of CD44 is a marker for activated and memory T cells in mice (11), and a population of activated T cells is able to bind HA (12). CD44 has the potential to provide costimulatory activity during T cell activation, as cross-linking CD44 together with the TCR increases proliferation and expression of activation markers, as well as augmenting IL-2 production (reviewed in Ref. 13). HA binding is induced upon T cell activation, and there is some evidence to suggest that HA can enhance CD3-mediated activation of human peripheral T cells (14). HA is synthesized and expressed by dendritic cells (15), and HA and HA oligosaccharides induce dendritic cell maturation in a CD44-independent, TLR-4-dependent manner (16, 17). Better established is a role for CD44 and HA in the extravasation of T cells to sites of inflammation. CD44 allows a mouse T cell line to roll on HA coated surfaces (18) and on TNF-α stimulated endothelial cells in vitro (19), with similar observations being made in vivo with Th1 and Th2 polarized cells (20). Rolling on endothelial cells is necessary for subsequent firm adhesion and extravasation of T cells, and CD44 has been shown to facilitate this process by enhancing VLA-4 mediated adhesion (21). Furthermore, T cell recruitment to inflammatory sites in staphylococcal enterotoxin B-induced peritonitis (22) and collagen-induced arthritis (8) is CD44-dependent.

There is also evidence that CD44 is involved in activation-induced cell death (AICD). AICD usually occurs following secondary stimulation of activated T cells that have experienced prolonged exposure to IL-2 and primarily involves the interaction of the death receptor Fas with Fas Ligand (FasL). The process of AICD, together with activated cell-autonomous death, is responsible for removal of activated T cells and maintenance of immune homeostasis (reviewed in Ref. 23). Nagarkatti's group has shown that T cells from CD44 null mice are less susceptible to apoptosis after conconavalin A stimulation and more resistant to TCR-stimulated AICD in vitro (24, 25). This was not due to increased Fas expression and occurred independently of Fas, as lymphoproliferative and autoimmune symptoms in mice lacking expression of both CD44 and Fas were exacerbated (26). However, another study using CD44 and Fas double null mice reported a reduction in lymphoproliferative symptoms when compared with Fas null mice (27). In addition, studies with human Jurkat T lymphoma cells and peripheral blood T cells have indicated that CD44 has the potential to affect Fas-dependent cell death (28, 29), and CD44 cross-linking can reduce apoptosis and AICD in T cell lines (30, 31). Thus the precise role of CD44 in AICD is not clear and the effect of the interaction with its physiological ligand, HA, has not been determined. In this study, we use two CD44 mutants that either increase or prevent HA binding to show that the interaction between CD44 and HA causes cell death in activated human Jurkat T cells. This HA-dependent cell death occurred independently of both Fas and caspases, and was observed in primary T cells in the absence of Fas-dependent apoptosis.

Department of Microbiology and Immunology, Life Sciences Institute, University of British Columbia, Vancouver, British Columbia, Canada

Received for publication June 2, 2008. Accepted for publication August 28, 2008.

The costs of publication of this article were defrayed in part by the payment of page charges. This article must therefore be hereby marked *advertisement* in accordance with 18 U.S.C. Section 1734 solely to indicate this fact.

[1] This work was supported by a grant from the Canadian Institutes of Health Research. B.R. was funded by the Heart and Stroke Foundation of Canada.

[2] Address correspondence and reprint requests to Dr. Pauline Johnson, Department of Microbiology and Immunology, University of British Columbia, 2350 Health Sciences Mall, Vancouver, British Columbia, V6T 1Z3, Canada. E-mail address: pauline@interchange.ubc.ca

[3] Abbreviations used in this paper: HA, hyaluronan; AICD, activation-induced cell death; β-D-xyloside, p-nitrophenyl β-D-xylopyranoside; CS, chondroitin sulfate; DAPI, 4′,6-diamidino-2-phenylindole; FasL, Fas ligand; Fl-HA, fluorescein-conjugated HA; PI, propidium iodide; PS, phosphatidylserine.

Materials and Methods

Cell lines

The human Jurkat T lymphoma cell line, clone E6.1, was purchased from the American Type Culture Collection (ATCC) and was cultured in RPMI 1640 supplemented with 10% FCS, 1 mM sodium pyruvate (Invitrogen), 2 mM L-glutamine (Sigma-Aldrich), and 50 U/ml Penicillin/Streptomycin (Invitrogen). To obtain CD44-positive cells, Jurkat cells were electroporated with 20 μg of CD44H-pCEP4 plasmid DNA using the Gene Pulser apparatus (Bio-Rad) at 250 V and 950 μF and selected in 300 μg/ml hygromycin B (Calbiochem). Cells were then sorted for high CD44 expression on a FACS Vantage SE Turbo (BD Biosciences). All experiments were performed with cells grown in the absence of selection for 3–10 days.

Abs and reagents

Purified rat anti-human/mouse CD44 mAb IM7.8.1 (ATCC no. TIB-235) was conjugated to Alexa 488 (Molecular Probes) or coupled to cyanogen bromide-activated Sepharose 4B (Amersham Biosciences) according to the manufacturer's instructions. The mouse anti-human CD44 mAb 3G12 was obtained from G. Dougherty (University of Arizona, Tucson, AZ) (32) and the mouse anti-human CD44 mAb Hermes-3 was obtained from the ATCC (no. HB-9480). Hermes-1, a rat anti-human CD44 mAb capable of blocking binding to HA, was purchased from the Development Studies Hybridoma Bank (University of Iowa, Iowa City, IA). The mouse anti-human TCR mAb C305 (no. CRL-2424) and anti-CD3 mAb OKT3 (no. CRL-8001) were obtained from the ATCC. The anti-chondroitin sulfate (CS) mAb 2B6 was purchased from Seikagaku America. The mouse anti-human Fas mAb DX2 was purchased from Southern Biotechnology Associates, whereas 7C11, an IgM mAb capable of inducing Fas-mediated apoptosis, was purchased from Immunotech. The mouse anti-human blocking mAb against Fas (ZB4) was obtained from Stressgen, whereas the mouse anti-human (NOK-1) and hamster anti-mouse (MFL3) blocking mAbs against FasL were obtained from eBioscience. Unlabeled goat anti-rat Ab and goat anti-mouse Ab were a gift from I. Trowbridge (Salk Institute, La Jolla, CA). FITC-conjugated goat anti-mouse Ab was purchased from Caltag Laboratories, and HRP-conjugated goat anti-mouse Ab was obtained from Jackson ImmunoResearch. Fluorescein-conjugated HA (Fl-HA) was made as described (33) using rooster comb HA obtained from Sigma-Aldrich. Prestained molecular mass standards were purchased from NEB, and the pan-caspase inhibitor z-VAD-fmk was obtained from Calbiochem.

Generation of point mutations

Human CD44H cDNA (34) in pCEP4 (Invitrogen) and S180A and G181A mutations in human CD44 were described previously (35). The R41A mutation was created by oligonucleotide site directed mutagenesis using four primers: primer 1 containing a *Nco*I site (forward, 5′-CGCTCCGGACAC CATGGACAAG-3′); primer 2 containing a *Hpa*I site (reverse, 5′-CGGGTGCCATCACGGTTAACAATAGT-3′); and complementary primers 3 (forward, 5′-AAAAATGGT*GC*CTACAGCATCTCTCGG-3′) and 4 (reverse, 5′-CCGAGAGATGCTGTAG*GC*ACCATTTTT-3′) containing the R41A mutation. The mutated sequences are italicized. Two fragments were generated by PCR using primers 1 with 4 and 2 with 3. The fragments were then mixed and PCR performed again. The final product was inserted into the CD44 sequence using *Nco*I and *Hpa*I.

Flow cytometry

Cells (2×10^5) were incubated with 1 μg/ml DX2 in PBS containing 2% FCS and 5 mM EDTA for 30 min on ice, washed once, and incubated with 10 μg/ml FITC-goat anti-mouse Ab. Alternatively, cells were incubated with ~5 μg/ml IM7-Alexa 488 or Fl-HA. After washing, cells were resuspended in buffer containing 1 μg/ml propidium iodide (PI; Sigma-Aldrich). A minimum of 5000 live events was collected on a FACScan and analyzed using CellQuest (BD Biosciences) or FlowJo (Tree Star) software.

Analysis of CS on CD44

Immunoprecipitation, sulfate labeling, and Western blotting of CD44 was performed as described (35). In brief, cells were cultured for 2 days in $Na_2[^{35}SO_4]$ following a 1 day incubation in the presence or absence of 2 mM p-nitrophenyl β-D-xylopyranoside (β-D-xyloside; Sigma-Aldrich). Cells were lysed and incubated with IM7-coupled beads. Some samples were digested with *Proteus vulgaris* chondroitinase ABC or *Flavobacterium heparinum* heparitinase (Seikagaku America). Immunoprecipitated CD44 was resolved on a 7.5% SDS polyacrylamide gel and transferred to a polyvinylidene fluoride membrane (Millipore). Membranes were exposed to Kodak BioMax MR film (Interscience) at −80°C for 3–10 days. To determine relative CD44 levels, membranes were blotted with 3G12. To detect CS, immunoprecipitated CD44 from 1×10^7 cells was digested with chondroitinase ABC to expose the epitope for the anti-CS mAb 2B6. Following sequential incubations with the 2B6 mAb and HRP-goat anti-mouse Ab, membranes were developed with ECL (Amersham Biosciences) according to the manufacturer's instructions.

Low molecular mass HA generation and analysis

HA was dissolved in 150 mM NaCl, 100 mM NaOAc, 1 mM EDTA, (pH 5.0) at a concentration of 5 mg/ml and bovine testes hyaluronidase (Calbiochem) was added at 200 U/ml. The mixture was incubated at 37°C for 10 s or 16 h before inactivation of the enzyme by boiling for 10 min, followed by adjustment of the pH to 7.0. HA was analyzed by PAGE and silver staining as described (36). From the observed pattern, HA digested for 10 s was termed intermediate molecular mass HA, whereas HA digested for 16 h was low molecular mass HA. To compare relative binding of CD44 to different sizes of HA a competitive binding assay was set up in which cells stimulated for 8 h with 10 ng/ml PMA (Sigma-Aldrich) were incubated with 0.5 μg/ml Fl-HA mixed with 0.5 μg/ml to 5 mg/ml unlabeled HA, intermediate HA, or low molecular mass HA on ice for 30 min. Cells were analyzed by flow cytometry as described above.

Cell death analysis

Cell viability was assessed by flow cytometry following labeling with PI and Annexin V-FITC (Southern Biotechnology Associates) according to the manufacturer's instructions. Annexin V-PE obtained from BD Biosciences was also used in one experiment. The percentage of viable cells was determined by the percent of cells negative for both Annexin V and PI. In one experiment, cells were labeled with PI alone and the number of live events collected in 30 s was counted. Data was normalized by setting the number of live events in the untreated sample to 100%. Caspase activation was determined by Western blotting to detect cleaved fragments with an anti-caspase 3 Ab or an anti-caspase 8 mAb purchased from Cell Signaling. Mitochondrial membrane polarization was measured using JC-1 (Molecular Probes) according to the manufacturer's instructions. Cell polarization was measured by labeling with $DiOC_6(3)$ (Calbiochem) at a final concentration of 40 nM followed by the addition of PI and analysis by flow cytometry. DNA fragmentation was measured using the TUNEL based FlowTACS kit obtained from R&D Systems according to the manufacturer's instructions. Chromatin condensation was assessed either by analysis of 4′,6-diamidino-2-phenylindole (DAPI; Invitrogen) labeled cells using an Olympus FluoView FV1000 laser scanning confocal microscope or by flow cytometry of cells labeled with a mouse IgM mAb against ssDNA (Chemicon) and PI according to the manufacturer's instructions.

Induction of cell death

Cells were suspended at 5×10^5 cells/ml and treated with 100 nM staurosporine (Sigma-Aldrich) or 10–100 ng/ml 7C11, an anti-Fas mAb, for various times. CD44 was cross-linked either by incubating cells with 10 μg/ml Hermes-1 or Hermes-3 for 20 min on ice, washing once, and culturing cells for 16 h with 10 μg/ml goat anti-rat or goat anti-mouse Ab, or by incubating cells for 0 to 8 h with both 5 μg/ml Hermes-1 and 25 μg/ml goat anti-rat Ab. Serum starvation was conducted by incubating 1×10^5 cells/ml in RPMI 1640 without FCS for 0 to 3 days.

Cell stimulation

Cells were suspended at 5×10^5 cells/ml in RPMI-10% FCS and stimulated with 10 ng/ml PMA for various times in the presence or absence of the mAbs Hermes-1 or Hermes-3 at 10 μg/ml. Alternatively, cells were added to 96-well plates coated with 50 μl of 5 μg/ml C305 or OKT3. To control the amount of HA in the culture medium, cells were resuspended in AIMV (Invitrogen), which is a defined serum-free media that does not contain HA. Various concentrations of HA, intermediate HA or low molecular mass HA along with 10 μg/ml Hermes-1 or 1 U/ml *Streptomyces* hyaluronidase (Calbiochem) were then added to the cells for 30 min before PMA stimulation for 16 h. Alternatively, cells were stimulated in AIMV for 12 h with PMA, and then incubated with or without blocking Abs or inhibitors for 20 min before the addition of various amounts of HA for up to 8 h.

FasL RT-PCR

RNA from ~4×10^6 cells was isolated using RNeasy Mini kit (Qiagen) and 10 μg was reverse transcribed with Superscript II (Invitrogen) according to the manufacturer's instructions. PCR using ~2.5 μg of cDNA was performed with *Taq*DNA polymerase in 50 μl with 1 mM Mg^{2+} as follows: 94°C for 2 min; 25–40 cycles at 94°C for 30 s, 58°C for 30 s, and

72°C for 50 s; 72°C for 10 min. β-actin primers (forward, 5′-GACTAC CTCATGAAGATCCT-3′; reverse, 5′-ATCCACATCTGCTGGAAGGT-3′) formed a 512 bp fragment and amplification was done for 25 cycles. FasL primers (forward, 5′-CACTACCGCTGCCACCCC-3′; reverse, 5′-CCAGAGAGAGCTCAGATACGTTG-3′) formed a 606 bp fragment, and amplification was done for 40 cycles. PCR product (20 μl) was electrophoresed in 1.5% agarose gel containing SYBR Safe (Invitrogen) and visualized under UV light.

Primary cells

Splenic T cells were purified from 6–12-wk-old C57BL/6 (The Jackson Laboratory) and $CD44^{-/-}$ mice (37) by negative selection. In brief, spleens were ground up using glass slides and RBC were lysed using 0.83% ammonium chloride. Cells were then suspended in PBS containing 2 mM EDTA and 0.5% BSA, and incubated with biotin-conjugated mAbs against B220, CD11b and Ter119, washed, then incubated with anti-biotin magnetic microbeads (Miltenyi Biotec). After washing, cells were run through a MACS LS separation column (Miltenyi Biotec) to remove non-T cells. Preparations were over 90% positive for CD3 expression immediately after purification and over 98% positive by day 6, as determined by flow cytometry. Fas negative T cells from MRL/*lpr* mice were purified as above, except that an anti-CD19 mAb was used in place of the B220 mAb. Following purification, cells at 10^6/ml were stimulated with 2.5 ng/ml PMA and 500 ng/ml ionomycin (Sigma-Aldrich) in complete RPMI 1640 with 10 mM HEPES and 55 μM 2-ME. After 2 days, 20 U/ml of IL-2 (R&D Systems) was added to the media and the cells were maintained in IL-2 at $1–2 \times 10^6$ cells/ml. On day 5, cells were resuspended at 1×10^6 cells/ml in AIMV with or without 1 μg/ml of the Fas blocking mAb MFL3 and added to wells coated with 0.1–5 μg/ml of the anti-CD3 mAb 2C11 and/or 5 μg/ml of the anti-CD44 mAb IM7 for 24 h. HA at 500 ng/ml was added to some samples at various times during stimulation. Cell viability and HA binding was assessed as described above. Animal experimentation was conducted in accordance with protocols approved by the University Animal Care Committee and Canadian Council of Animal Care guidelines.

Statistics

Data are shown as the mean ± SD of three experiments, unless otherwise indicated. Significance was determined by the Student's *t* test. *, $p < 0.05$, **, $p < 0.01$, ***, $p < 0.001$.

Results

CS addition to CD44 regulates HA binding in Jurkat T cells

To evaluate the effect of HA binding in T cells, CD44 negative Jurkat T lymphoma cells were transfected with human CD44 or CD44 containing S180A or R41A point mutations. R41, located within the HA binding site, is critical for HA binding and mutation to an alanine abolishes HA binding (38, 39). The S180A mutation acts as a gain-of-function mutant as it prevents CS addition and increases the affinity of CD44 for HA when made as an Ig-fusion protein or when expressed in mouse fibroblast L cells (35). However, it was not known whether CS modification negatively regulates HA binding in T cells. To first determine whether S180A-CD44 could be used as a constitutive HA binding mutant in T cells, HA binding was assessed in the transfected cells. Levels of CD44 expression were approximately equivalent, yet S180A-CD44 expressing cells bound significantly higher levels of Fl-HA compared with wild-type CD44, as determined by flow cytometry (Fig. 1*A*). Stimulation of CD44 transfected Jurkat cells with 10 ng/ml of PMA for 8 h induced HA binding in CD44 expressing cells and further enhanced binding in S180A-CD44 expressing cells, whereas R41A-CD44 transfected cells did not bind HA under any condition tested. This suggested that CS addition to CD44 was reducing HA binding in Jurkat T cells.

To confirm CS modification of residue S180, CD44 was immunoprecipitated from cells grown in the presence of sodium [^{35}S]sulfate (Fig. 1, *B* and *C*). Although CD44 did not display the heavily sulfated, heterogeneous, high molecular mass forms normally indicative of large chain CS addition, sulfate incorporation by CD44 was reduced by growth in the presence of β-D-xyloside, an inhibitor of glycosaminoglycan addition, and by treatment with

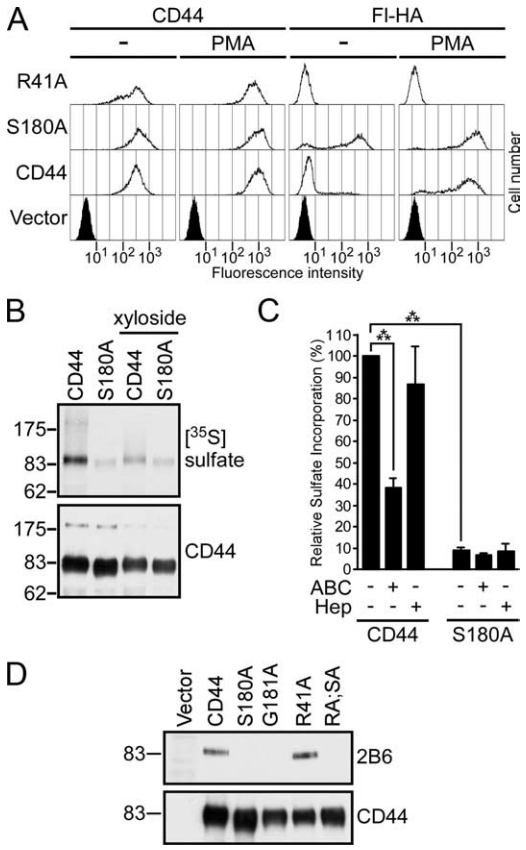

FIGURE 1. S180A mutation in CD44 prevents CS addition and results in constitutive HA binding in Jurkat cells. *A*, CD44 expression and HA binding were analyzed by flow cytometry in transfected Jurkat cells either unstimulated or stimulated for 8 h with PMA. The two *left panels* show expression levels of CD44, detected using Alexa 488 conjugated IM7, whereas the two *right panels* show binding to Fl-HA. *B*, CD44 immunoprecipitated from sodium [^{35}S]sulfate-labeled cells grown in the presence or absence of β-D-xyloside and resolved by SDS-PAGE. *C*, Relative quantitation of sulfate incorporation by CD44 before and after digestion with chondroitinase ABC (ABC) or heparitinase (Hep) as measured by densitometry. Sulfate incorporation by untreated wild-type CD44 was set to 100% after adjustment for the level of CD44. Data are shown as the mean ± SD of three experiments with significance determined by the Student's *t* test (***, $p < 0.001$). *D*, Detection of CS on immunoprecipitated CD44 by Western blotting with the anti-CS mAb 2B6. CD44 loading levels were determined by blotting with the mAb 3G12.

chondroitinase ABC. This suggested that CD44 in Jurkat T cells is modified by short chains of CS. Wild-type CD44 was sulfated to a much greater extent than S180A-CD44, which was also unaffected by β-D-xyloside or chondroitinase ABC, indicating that S180 is the major site of CS addition. This was further supported by Western blotting CD44 with the anti-CS mAb 2B6 (Fig. 1*D*), which bound to wild-type and R41A-CD44, but not to CD44 containing either the S180A or G181A mutations that prevent CS addition (35). Together, these data indicate that CS addition occurs on CD44 in Jurkat T cells and negatively regulates HA binding. Notably, even low molecular mass forms of CS on CD44 are able to exert this effect.

High HA binding T cells are more susceptible to AICD

The generation of Jurkat cells expressing CD44 with different binding abilities for HA (high, low, and not detectable) allowed us to investigate the consequences of HA binding. Stimulation with immobilized TCR mAb induced cell death in both Jurkat T cells

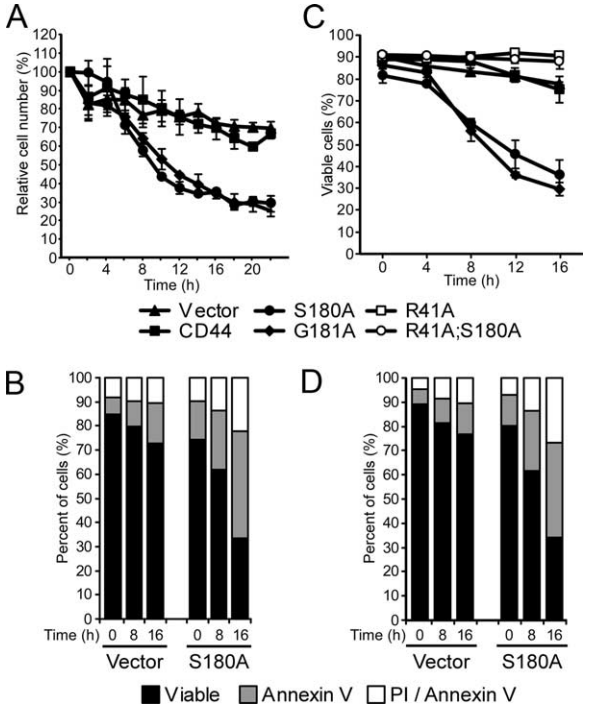

FIGURE 2. Cell death is preferentially induced in TCR- or PMA-stimulated Jurkat cells expressing a high HA binding form of CD44. *A*, Time course showing percentage of live cells after stimulation with the anti-TCR mAb C305. Data are shown as the mean ± SD of three experiments and were normalized by setting the number of live events in the untreated samples to 100%. *B*, Representative experiment showing the percentage of cells that were unstained (viable), single positive for Annexin V, or double positive for both Annexin V and PI following anti-TCR stimulation. *C*, Time course of cell viability during PMA stimulation as determined by lack of Annexin V-FITC and PI staining. Data are shown as the mean ± SD of three experiments. *D*, Same as *B*, except cells were stimulated with PMA.

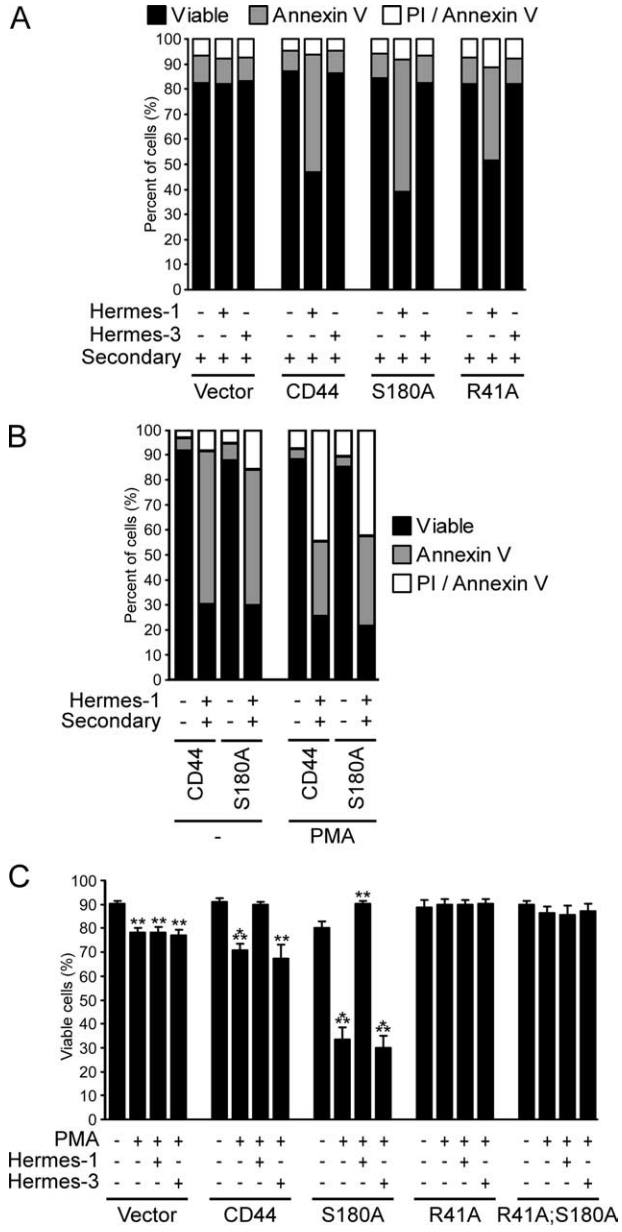

FIGURE 3. CD44 mAbs can induce or prevent cell death of transfected Jurkat cells during PMA stimulation. *A*, Representative experiment showing the percentage of cells that were viable, single positive for Annexin V, or double positive for both Annexin V and PI following incubation with Hermes-1 or Hermes-3 for 20 min and cross-linking with secondary Ab for 16 h. *B*, Same as *A*, except unstimulated or PMA stimulated cells were grown in AIMV serum-free media before coincubation of Hermes-1 and secondary Ab for 8 h. *C*, Graph showing percentage of viable cells following PMA stimulation for 16 h in the presence or absence of the HA blocking anti-CD44 mAb Hermes-1 or the nonblocking anti-CD44 mAb Hermes-3. Data are shown as the mean ± SD of three experiments with significance determined by the Student's *t* test (**, $p < 0.01$, ***, $p < 0.001$).

and CD44 expressing Jurkat T cells; however, this AICD was noticeably more pronounced in both S180A-CD44- and G181A-CD44 expressing cells (Fig. 2*A*). A subset of Annexin V single positive cells, most noticeable in the S180A-CD44 expressing cells, indicated that phosphatidylserine (PS) exposure was occurring either before, or in the absence of, cell death (Fig. 2*B*). PMA stimulation protects Jurkat cells from Fas-dependent apoptosis (40) and in accordance with this, minimal cell death was observed in vector control and wild-type CD44 transfectants following PMA stimulation (Fig. 2*C*). However, Annexin V binding and cell death was still observed in cells expressing the high HA binding S180A-CD44 mutant (Fig. 2*D*). Enhanced survival, not death, was observed in cells expressing either R41A-CD44 or R41A;S180A-CD44, suggesting that it is the ability to bind HA, not the loss of CS addition, that is a factor in PMA-induced T cell death (Fig. 2*C*). The data showed a good correlation between the HA binding ability of CD44 and the degree of cell death observed during the activation of Jurkat cells with anti-TCR mAb or PMA. Furthermore, as PMA activation protects against Fas-mediated apoptosis in Jurkat cells, it suggests that this cell death may occur independently of Fas.

HA binding by CD44 enhances AICD in T cells

To verify that all mutant forms of CD44 had a similar capacity to induce PS exposure and cell death, all forms of CD44 were cross-linked with Hermes-1, a mAb that binds to the HA binding site of CD44. This induced equal amounts of Annexin V and PI staining from all CD44-expressing cells in unstimulated and PMA stimulated Jurkat T cells (Fig. 3, *A* and *B*). More cell death was noted after PMA stimulation (Fig. 3*B*), and CD44 cross-linking with Hermes-3, a CD44 mAb that does not bind to the HA binding site, did not induce PS exposure (Fig. 3*A*). This suggested that HA binding may cross-link CD44 and induce AICD in the PMA-stimulated Jurkat T cells. To further evaluate this possibility, soluble

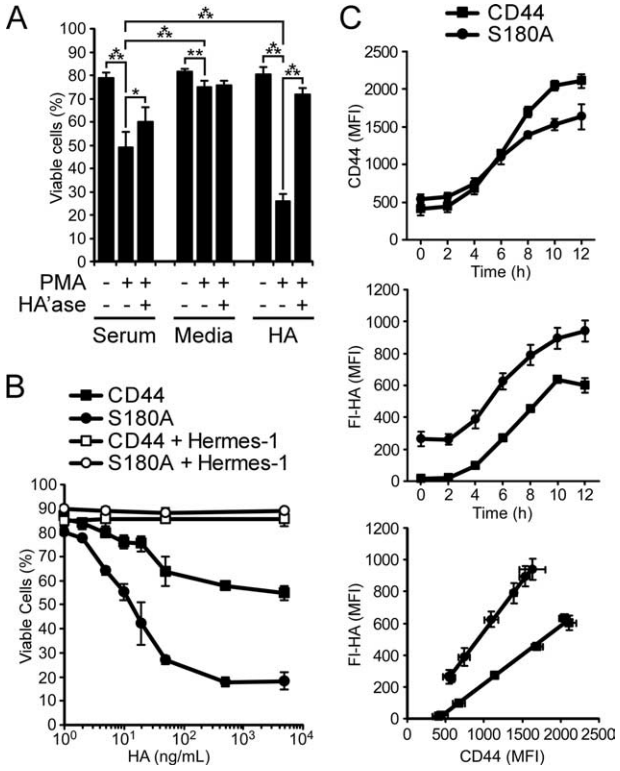

FIGURE 4. Enhanced AICD in Jurkat transfectants is dependent upon HA binding by CD44. *A*, Graph showing cell viability in S180A-CD44 cells following PMA stimulation for 16 h in RPMI 1640 supplemented with 10% FCS or in RPMI 1640 with or without 5 μg/ml HA. Hyaluronidase (HA'ase) treatment was done for 30 min before PMA stimulation. Data are shown as the mean ± SD of three experiments with significance determined by the Student's *t* test (*, $p < 0.05$, **, $p < 0.01$, ***, $p < 0.001$). *B*, Cell viability is shown following PMA stimulation for 16 h in AIMV serum-free media with various concentrations of HA. The HA-blocking anti-CD44 mAb Hermes-1 was added to some samples. *C*, The mean fluorescence intensity (MFI) for CD44 and S180A-CD44 expression (*top panel*) and Fl-HA binding (*middle panel*) at various time points during PMA stimulation is shown. The *bottom panel* shows the relationship between Fl-HA binding and the level of CD44 expression for CD44 and S180A-CD44. Data in *B* and *C* are shown as the mean ± SD of three experiments.

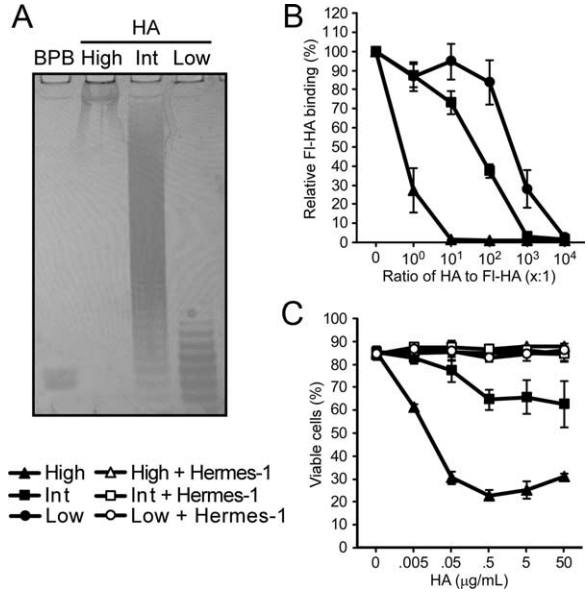

FIGURE 5. The size of HA affects its ability to induce cell death in PMA-stimulated cells. *A*, Visualization of high, intermediate (int), or low molecular mass HA by silver staining samples run on a 15% acrylamide gel. Bromophenol blue (BPB) was used as a marker dye. *B*, Competition assay between Fl-HA and increasing amounts of unlabeled high, intermediate, and low molecular mass HA in S180A-CD44 cells. *C*, Cell viability is shown in S180A-CD44 cells following PMA stimulation for 16 h in AIMV serum-free media with various concentrations of high, intermediate, or low molecular mass HA. The HA-blocking anti-CD44 mAb Hermes-1 was added to some samples. Data in *B* and *C* are shown as the mean ± SD of three experiments.

Hermes-1 and Hermes-3 mAbs were added to cells during PMA stimulation. Hermes-1 completely prevented cell death induced by PMA stimulation in S180A-CD44 and wild-type CD44 cells, whereas Hermes-3 had no effect (Fig. 3*C*). These results strongly suggest that the binding of serum HA by wild-type and S180A-CD44 enhances cell death during PMA stimulation. Unexpectedly, the small amount of death observed in the vector control cells as a result of PMA stimulation was not observed in the CD44-R41A transfectants (Fig. 3*C*). This implies that the inability of CD44 to bind HA protects against cell death, whereas high HA binding forms of CD44 promote cell death.

As Jurkat T cells do not produce HA (41), the likely source of HA in these experiments was the FCS present in the media. To examine this, 500 ng/ml of HA purified from rooster comb was added to CD44-S180A transfectants cultured in medium without FCS. In the absence of FCS, only a small amount of cell death occurred following PMA stimulation for 16 h, whereas the addition of HA greatly increased cell death (Fig. 4*A*). This was not due to contaminants in the purified HA, as cell death was prevented by digestion of the HA with hyaluronidase before PMA stimulation. Titration of purified HA into serum-free AIMV media revealed that concentrations as low as 10 ng/ml augmented AICD significantly in both CD44 and S180A-CD44 transfectants, with the maximum amount of cell death occurring with HA concentrations below 500 ng/ml (Fig. 4*B*). CD44 and HA dependency was demonstrated by the ability of Hermes-1 mAb to completely block death from occurring, even in the presence of 5000 ng/ml of HA. Therefore, the data show that HA binding by both wild type and mutant CD44 results in a substantial increase in AICD upon PMA stimulation of Jurkat transfectants.

Analysis of CD44 expression and HA binding in CD44 and S180A-CD44 expressing cells revealed a time-dependent increase in both upon PMA stimulation (Fig. 4*C*). HA binding was significantly induced in wild-type CD44 transfectants and increased in S180A-CD44 transfectants such that HA binding was always greater in S180A-CD44-expressing cells (Fig. 4*C*, *middle panel*). Furthermore, S180A-CD44 expressing cells showed consistently higher HA binding when equivalent CD44 levels were compared (Fig. 4*C*, *lower panel*), suggesting that cells expressing this mutated form of CD44 have a higher overall avidity for HA than those expressing wild-type CD44.

The size of HA affects its ability to enhance cell death

HA in the extracellular matrix normally consists of high molecular mass chains ($>10^6$ Da), but in inflamed tissues HA is degraded and lower molecular mass HA fragments can be detected. These smaller forms of HA have been shown to be proinflammatory when added to dendritic cells or macrophages (reviewed in Ref. 5). It was therefore of interest to determine whether the size of HA could affect its ability to enhance AICD in T cells. To generate intermediate or low molecular mass HA, bovine testicular hyaluronidase was used to digest HA (Fig. 5*A*). Both intermediate and

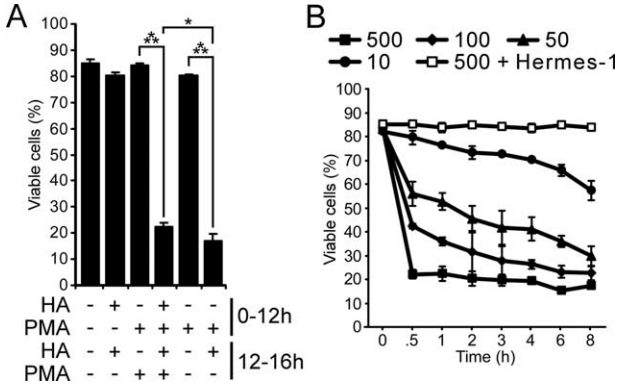

FIGURE 6. HA can rapidly induce cell death in CD44-expressing cells after PMA activation. *A*, Graph showing cell viability in S180A-CD44 cells suspended in AIMV media and stimulated with PMA in the presence or absence of 500 ng/ml HA. Cells were initially stimulated for 12 h, then washed twice and incubated for an additional 4 h in the presence of PMA and/or HA. Data are shown as the mean ± SD of three experiments with significance determined by the Student's *t* test (*, $p < 0.05$, ***, $p < 0.001$). *B*, Time course of cell viability following the addition of HA to S180A-CD44 cells prestimulated for 12 h with PMA. Hermes-1 mAb was added 20 min before the addition of HA for one sample set. Data are shown as the mean ± SD of three experiments.

low molecular mass HA displayed an ability to compete for Fl-HA binding to CD44 (data not shown) and S180A-CD44 (Fig. 5*B*). Although unlabeled HA effectively competed with Fl-HA when used in 10-fold excess, a 1,000-fold excess was required for intermediate, and a 10,000-fold excess for low molecular mass HA. During PMA stimulation 500 ng/ml of intermediate-sized HA caused significant death in S180A-CD44 cells. However, cell death was only a fraction of the cell death observed with high molecular mass HA, even when the concentration was increased as high as 50 μg/ml (Fig. 5*C*). Low molecular mass HA did not affect viability at any concentration tested. This experiment demonstrates that the size of HA is important in determining its ability to enhance AICD.

HA rapidly induces cell death in PMA stimulated Jurkat T cells

As CD44 cross-linking has been reported to provide costimulatory activity during T cell activation (13, 42), it was possible that the HA-mediated augmentation of cell death observed during the activation of Jurkat cells was due to HA providing a costimulatory signal through CD44 and enhancing T cell activation. To determine whether the HA signal had to be given simultaneously with the TCR or PMA signal, CD44-S180A cells were stimulated with PMA for 12 h, washed twice, and then incubated with HA for 4 h (Fig. 6*A*). Incubation of cells with HA for 4 h subsequent to PMA stimulation had the same effect on cell viability as incubation with both HA and PMA for

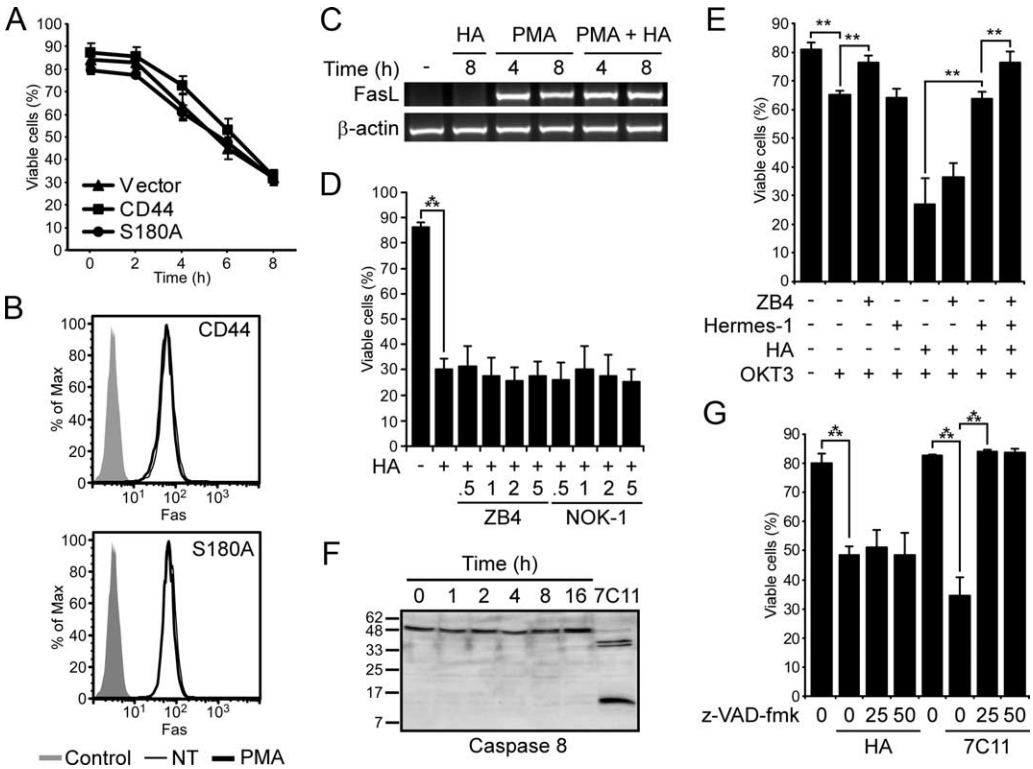

FIGURE 7. HA-induced cell death does not occur via the Fas/FasL pathway. *A*, Cell viability was assessed in unstimulated cells incubated with the anti-Fas mAb 7C11 for various times. Data are shown as the mean ± SD of three experiments. *B*, Fas expression as determined by flow cytometry in cells cultured in 10% FCS and either stimulated with PMA for 8 h or left untreated (NT). *C*, FasL mRNA expression in AIMV-cultured S180A-CD44 cells as determined by semiquantitative PCR following PMA stimulation in the presence or absence of HA. β-actin was used as a loading control. *D*, Cell viability of S180A-CD44 transfectants following the addition of HA for 2 h to cells prestimulated with PMA. Cells were preincubated for 20 min with the Fas-blocking mAb ZB4 or the FasL-blocking mAb NOK-1 before the addition of HA. *E*, Cell viability of S180A-CD44 cells activated for 16 h with immobilized anti-CD3 mAb OKT3 in the presence of various combinations of HA, ZB4, or Hermes-1. *F*, Western blot analysis of caspase 8 activation following the addition of HA to PMA-stimulated S180A-CD44 cells. Incubation of unstimulated cells with the anti-Fas mAb 7C11 for 2 h was used as a positive control. *G*, Same as *D*, except cells were preincubated for 20 min with 25 or 50 μM of the pan-caspase inhibitor z-VAD-fmk. As a control, unstimulated cells were incubated with z-VAD-fmk before the addition of the 7C11 mAb. For *D*, *E*, and *G* data are shown as the mean ± SD of three experiments with significance determined by the Student's *t* test (**, $p < 0.01$, ***, $p < 0.001$).

16 h. Cell death following the addition of HA occurred rapidly within 30 min, with the degree and time of cell death dependent on the amount of HA being added (Fig. 6*B*). These data demonstrate that HA binding induces cell death, and that this is not due to costimulation, but instead occurs independently in activated cells capable of binding high levels of HA.

HA-induced cell death occurs independently of Fas- and caspase-mediated apoptosis

Fas-susceptible Jurkat T cells become resistant to Fas-mediated apoptosis upon PMA stimulation (40), despite an up-regulation of FasL (43). It was therefore possible that HA binding by CD44 was causing cell death in Jurkat cells by reversing the effects of PMA on Fas signaling or otherwise inducing Fas signaling. In unstimulated cells, neither CD44 expression (Fig. 7*A*) nor the presence of exogenous HA (data not shown) affected sensitivity to apoptosis induced with an anti-Fas mAb. The expression of Fas (Fig. 7*B*) and FasL mRNA (Fig. 7*C*) were also unaffected by the presence of HA, although, as expected, FasL mRNA was increased by PMA stimulation. As these results did not rule out an effect of HA on the Fas signaling pathway, HA was also added to PMA-activated cells pretreated with blocking mAbs against Fas (ZB4) or FasL (NOK-1). Neither mAb had an effect on HA-induced cell death (Fig. 7*D*), indicating that HA was not acting via the Fas/FasL interaction. This was further confirmed by anti-CD3 activation of S180A-CD44 expressing Jurkat cells with various combinations of HA or blocking mAbs (Fig. 7*E*). Although blocking Fas largely prevented cell death in the absence of HA, it had minimal effect on HA-induced cell death. Notably, blocking Fas consistently reduced cell death in activated cells by ~10%, whereas blocking the CD44-HA interaction reduced cell death by an additional 30%. This indicates that HA- and Fas-dependent cell death are additive and suggests that the two signaling pathways are distinct. In support of this, the addition of HA to PMA stimulated cells did not result in the activation of caspase 8 (Fig. 7*F*), and even high concentrations of the pan-caspase inhibitor zFAD-fmk failed to inhibit HA-induced cell death (Fig. 7*G*).

Although AICD occurs primarily through the extrinsic Fas-dependent apoptotic pathway, the intrinsic mitochondrial-dependent pathway can also play a role (44). This is particularly true in Jurkat T cells, where even effective Fas signaling requires the mitochondrial pathway (45). As CD44 did not appear to be enhancing AICD via the extrinsic pathway, we investigated whether CD44 expression enhanced cell death via the intrinsic pathway. Death induced by either staurosporine or serum withdrawal was equal between the different Jurkat transfectants (Fig. 8*A*), with the addition of exogenous HA having no effect on apoptosis (data not shown). More importantly, membrane depolarization during HA-induced cell death was not detected before loss of membrane integrity, as measured with the mitochondrial specific JC-1 probe (Fig. 8*B*). Similar results were obtained with the more general $DiOC_6(3)$ probe (Fig. 8*C*), with depolarization only observed in cells that were positive with PI. Caspase 3 activation, which can result from cytochrome C release from the mitochondria, was also not observed following the addition of HA (Fig. 8*D*). These results indicate that HA-induced cell death in activated Jurkat cells does not activate this intrinsic, mitochondrial-dependent, apoptotic pathway.

The absence of caspase 3 and 8 activation and the failure of a pan-caspase inhibitor to block HA-induced cell death, suggested that CD44 induces a form of nonapoptotic programmed cell death. It has been proposed that caspase-independent cell death can be subdivided into either apoptotic-like or necrotic-like cell death depending upon the degree of chromatin condensation (reviewed in Ref. 46). Analysis of DAPI-labeled cells by confocal microscopy did not detect significant chromatin condensation in cells that had undergone HA-induced cell death, whereas it was apparent in cells that had undergone Fas-dependent apoptosis (Fig. 9*A*). To quantify the degree of chromatin condensation, cells were heated in the presence of formamide, which causes denaturation and ssDNA formation only in condensed chromatin (47), and then labeled with a mAb against ssDNA (Fig. 9*B*). A large proportion of cells treated with the anti-Fas mAb were positive for ssDNA, whereas only a small percentage of untreated, necrotic, or PMA stimulated cells were positive. Notably, there was an increase (8 ± 1%) in the percent of cells positive for ssDNA after HA and PMA stimulation for 16 h, but this was small compared with the percent of Annexin V positive cells (Fig. 9*C*). Approximately 40% of the HA stimulated cells had reduced cell volume, an event observed in the majority of cells undergoing Fas-mediated apoptosis (Fig. 9*D*). Consistent with the limited amount of chromatin condensation,

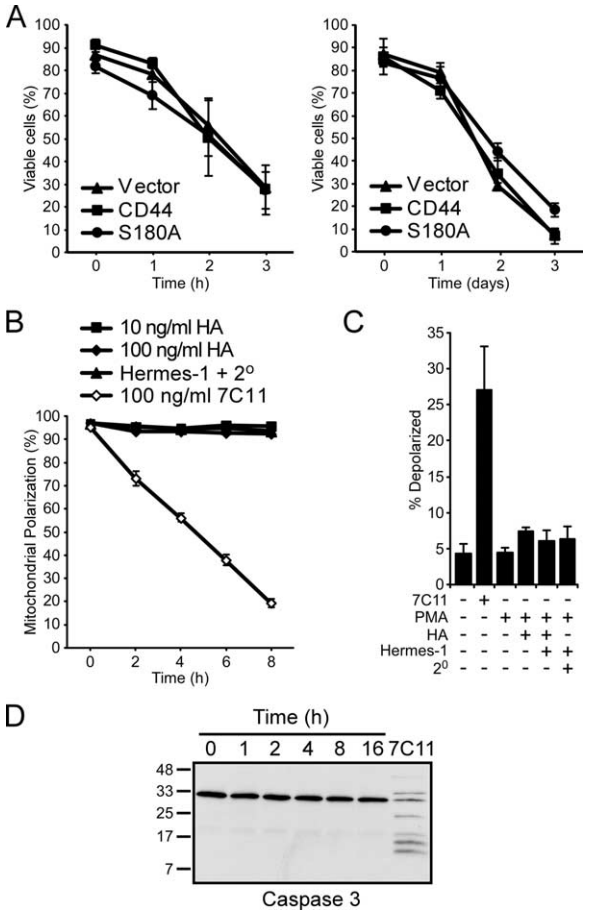

FIGURE 8. HA-induced cell death does not occur via the mitochondrial pathway. *A*, Cell viability of unstimulated Jurkat transfectants incubated with staurosporine for 1–3 h (*left panel*) or incubated in RPMI 1640 without FCS for 1–3 days (*right panel*). *B*, Time course of mitochondrial depolarization in S180A-CD44 cells. PMA-stimulated cells were incubated with either HA or Hermes-1 mAb and goat anti-rat Ab (2°) and then labeled with the mitochondrial membrane-specific dye JC-1. Incubation of unstimulated cells with the 7C11 mAb was used as a positive control. *C*, Same as *B*, except cells were analyzed after 2 h with the membrane dye $DiOC_6(3)$ and the percentage of live depolarized cells (PI negative, $DiOC_6(3)$ low) is shown. *D*, Western blot analysis of caspase 3 activation following the addition of HA to PMA-stimulated S180A-CD44 cells. Data from *A*, *B*, and *C* are shown as the mean ± SD of three experiments.

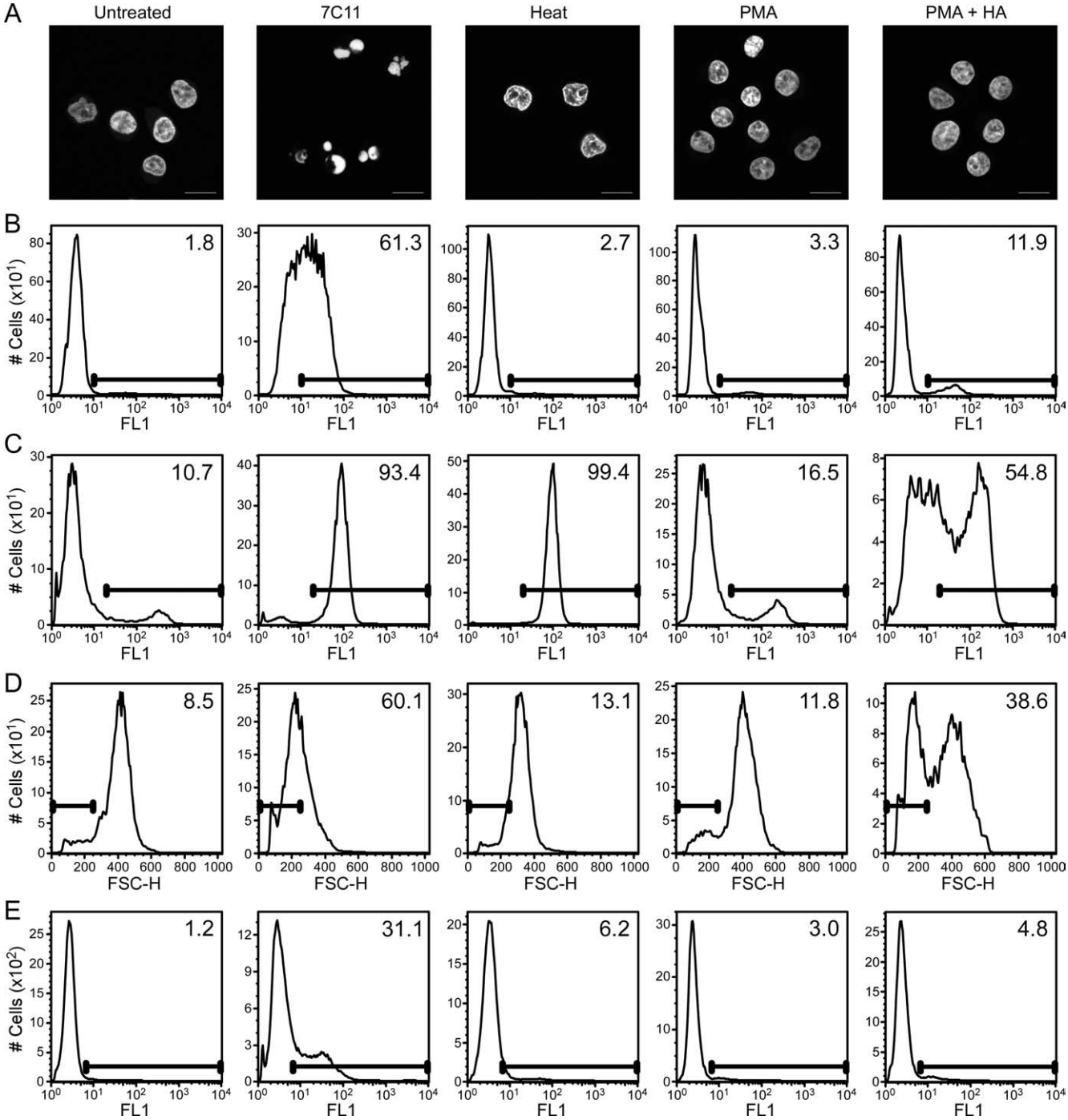

FIGURE 9. HA-induced cell death occurs in the absence of significant chromatin condensation or DNA fragmentation. Cells were PMA stimulated for 16 h with or without 500 ng/ml of HA. Apoptosis was induced with the anti-Fas mAb 7C11 for 16 h and necrotic cells were generated by heating cells at 56°C for 1 h. *A*, Confocal microscopy of DAPI-labeled cells. An optical section of 0.19 μm thickness is shown with the scale bar representing 10 μm. *B*, *C*hromatin condensation in diploid cells measured by flow cytometry using a mAb that recognizes ssDNA following heat denaturation in the presence of formamide. *C*, Annexin V labeling measured by flow cytometry. *D*, Cell size measured by flow cytometry. *E*, DNA fragmentation detected by TUNEL. The number of cells (#) is indicated on the *y*-axis in *B–E* and fluorescent intensity (FL1) on a log scale or size (FSC-H) is indicated on the *x*-axis in *B*, *C*, *E*, or *D*, respectively. The percentage of positive cells is indicated in each panel. One of three representative experiments is shown.

DNA fragmentation measured via the TUNEL assay (Fig. 9*E*) was not increased during HA-induced cell death. These data further show that HA-induced cell death is distinct from Fas-mediated or classical apoptosis involving caspase activation and chromatin condensation. Although HA induced certain characteristics consistent with apoptotic cell death such as decreased cell volume and increased PS exposure, HA-induced cell death appears to be most appropriately classified as necrosis-like programmed cell death.

CD44 and HA can mediate AICD in ex vivo T cells

Although AICD occurs upon TCR-mediated stimulation of Jurkat T cells, it requires secondary TCR stimulation preceded by culture in IL-2 in ex vivo T cells (48). This has led to the development of

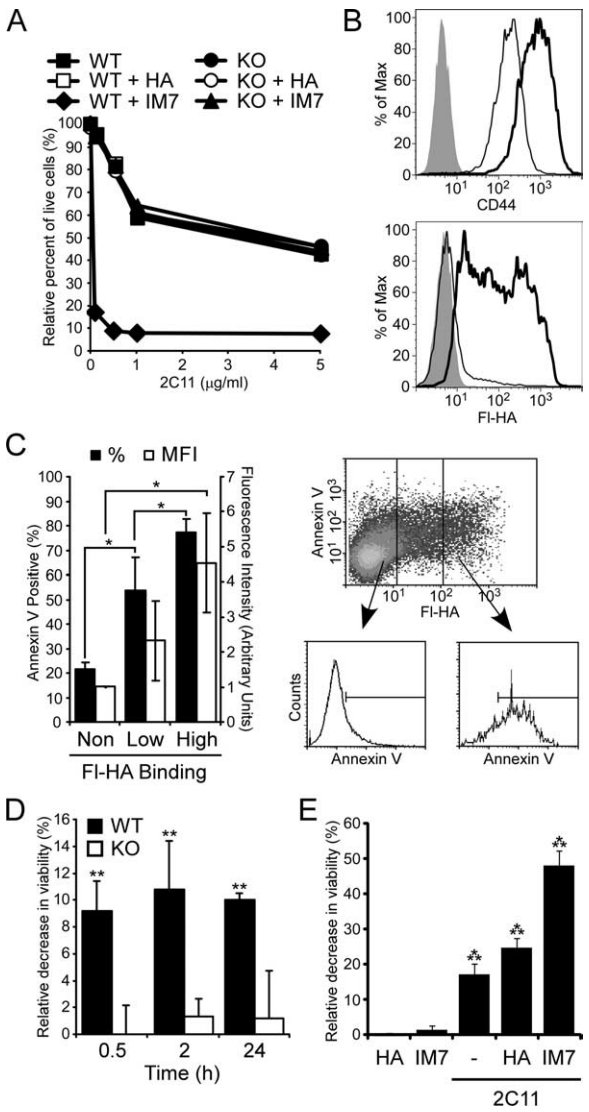

FIGURE 10. AICD in ex vivo activated murine splenic T cells is enhanced by the presence of HA. *A*, Representative experiment showing the percentage of live day 6 splenic T cells from wild-type (WT) and CD44 knockout (KO) mice following reactivation with immobilized anti-CD3 mAb 145-2C11 for 24 h (see *Materials and Methods* for details). Some samples were incubated with 500 ng/ml HA or with both immobilized anti-CD3 and anti-CD44 (IM7). The mean of three experiments is shown. *B*, Analysis of CD44 expression and Fl-HA binding of day 6 activated splenic T cells either unstimulated (thin line) or restimulated (thick line) for 24 h. The cells alone negative control (shaded) is also shown. *C*, Analysis of PS exposure and Fl-HA binding in day 6 wild-type splenic T cells. After restimulation for 24 h with 2.5 μg/ml of immobilized anti-CD3 mAb, cells were incubated with Fl-HA for 30 min at 37°C, labeled with Annexin V-PE on ice, and then analyzed by flow cytometry. Live cells were divided into non-, low-, and high-HA binding populations and analyzed for levels of Annexin V-PE binding. The percent of cells positive for Annexin V within each population is indicated. Mean fluorescence intensity (MFI) was normalized between experiments by setting the intensity of the non-HA binding population to 1, and data are shown as the mean ± SD of three experiments with significance determined by the Student's *t* test (*, $p < 0.05$). *D*, Graph showing the relative decrease in cell viability in day 6 T cells incubated in the presence of 1 μg/ml of the Fas blocking mAb MFL3 for 24 h on immobilized anti-CD3 mAb. HA at 500 ng/ml was added to the cells for 0.5 h, 2 h, or 24 h. To normalize between experiments, the percentage of loss of cell viability between cells stimulated in the absence vs the presence of HA is shown. Data are the mean ± SEM of four experiments with pools of two mice per experiment. Significance (**, $p < 0.01$) is shown compared with CD44 knockout (KO) cells. *E*, Graph showing the relative decrease in cell viability in Fas-negative T cells from MRL/*lpr* mice that were cultured and stimulated as in *A*. The data shown are the mean ± SEM of three experiments with a total of six mice. Significance (***, $p < 0.001$) is shown compared with the preceding sample.

an in vitro system for studying AICD where T cells are activated and then incubated for several days in IL-2 before restimulation. Using this procedure we determined whether HA was able to induce cell death in activated splenic T cells purified from wild-type C57BL/6 or CD44$^{-/-}$ mice. Equal amounts of death were observed after restimulation with immobilized anti-CD3 between wild-type and CD44 null cells, and the addition of HA had no effect (Fig. 10*A*). However, cell death was greatly enhanced when wild-type T cells were activated in the presence of immobilized anti-CD44 mAb IM7. Increased death was observed even with low concentrations of immobilized anti-CD3, yet there was no effect when the cells were not stimulated. This shows that CD44 can significantly augment AICD. However, this was not observed with HA, suggesting that the level of HA binding by restimulated T cells may be insufficient to induce significant cell death. Although the levels of CD44 were increased upon restimulation, the activated T cells showed a range of HA binding (Fig. 10*B*). To determine whether HA augmented AICD in the high HA binding cells, T cells were stimulated with suboptimal levels of anti-CD3, then incubated with Fl-HA for 30 min at 37°C, and finally labeled with Annexin V-PE. Analysis of live cells revealed that Fl-HA binding cells were also positive for Annexin V (Fig. 10*C*). Fl-HA binding cells were not Annexin V positive after primary stimulation of T cells (data not shown). Because we had previously found in the Jurkat T cells that HA-induced cell death occurred independently of Fas-dependent cell death, and given that the high HA binding population represented only a fraction of the activated T cells, we set out to determine whether HA-induced cell death could be observed more readily in the absence of Fas-dependent cell death. Fas-mediated AICD was blocked with an anti-FasL mAb added before stimulation and a comparison of cells stimulated in the presence vs the absence of HA revealed approximately a 10% reduction in the percent of viable cells (Fig. 10*D*). This decrease was not observed when HA was added to CD44$^{-/-}$ T cells. Death occurred within 30 min of adding HA to the T cells, recapitulating the timeframe observed in Jurkat T cells. Furthermore, CD44- and HA-dependent cell death was observed when AICD was induced in splenic T cells from MRL/*lpr* mice, which lack functional Fas (Fig. 10*E*). This demonstrates that HA-induced cell death occurs independently of Fas in a subset of activated T cells.

Discussion

In this study we have shown that HA induces cell death in activated T cells via CD44. HA-induced cell death was dependent on the ability of CD44 to bind HA, as a loss-of-function mutation in CD44 prevented cell death and a gain-of-function mutation increased cell death. Inhibition of HA-induced cell death by soluble CD44 mAbs and the induction of cell death by CD44 cross-linking suggest that the ability of HA to cross-link CD44 is an important factor in its function. This is also supported by the fact that intermediate to low molecular mass HA had a decreased ability to induce cell death. However, CD44 cross-linking with mAbs has previously been shown to decrease AICD (30, 31). These conflicting results may be due to the type or state of the cell examined, as we have shown that the outcome of CD44 ligation can depend on the activation state of the cell. CD44 cross-linking caused PS exposure in both unstimulated and PMA stimulated Jurkat T cells, yet significant cell death only occurred in activated cells. This

demonstrates that activation is required to make the cells susceptible to CD44-dependent cell death. Similarly, S180A-CD44 expressing Jurkat T cells bound HA constitutively, yet HA only induced cell death in PMA activated cells, again indicating that cells must first be activated to become susceptible to HA-induced cell death. This corresponds well to our observations with activated splenic T cells, in which neither incubation on immobilized anti-CD44 mAb nor the presence of HA induced cell death unless the cells were reactivated via the TCR. Furthermore, there was a correlation between the extent of HA binding and the percentage of cells showing PS exposure following secondary, but not primary, stimulation. This indicates that HA-induced cell death only occurs in T cells primed to undergo AICD.

This requirement of secondary activation for T cells to be susceptible to HA-dependent AICD is also observed for Fas-dependent AICD (23). Despite this, we found that Fas and HA acted independently to induce AICD. This was demonstrated most clearly in transfected Jurkat cells where both anti-Fas and anti-CD44 mAbs were required to completely block cell death. HA induced more AICD than Fas in activated $CD44^+$ Jurkat T cells, whereas the opposite appeared to be true in reactivated splenic T cells. This may relate to the extent of HA binding in activated T cells, as CD44-dependent AICD induced with immobilized CD44 mAbs was dramatic in both cell types. CD44 cross-linking can increase surface expression of FasL in human peripheral blood T cells (29). However, the independence of these two pathways during AICD in mice was demonstrated using MRL/*lpr* T cells that lack functional Fas, but were still susceptible to CD44 and HA-dependent AICD. This independence is also observed in vivo where the loss of CD44 increased the severity of lymphoproliferative and autoimmune disease in Fas deficient (*lpr/lpr*) mice (26).

Caspase-independent death has been previously described in an erythroleukemia cell line following treatment with an anti-CD44 mAb (49). In this case, death was linked to release of apoptosis-inducing factor and activation of calpain. However, we did not see mitochondrial depolarization, which is necessary for the release of apoptosis-inducing factor (reviewed in Ref. 50), and HA-induced cell death occurred in a much shorter time frame. Caspase-independent cell death has also been reported after cross-linking of CD2 (51), CD45 (52), CD47 (53), and CD99 (54). Although both CD45 and CD47 cross-linking induced mitochondrial depolarization, many similarities with CD44 were observed including a rapid onset of PS exposure, cell shrinkage, loss of membrane integrity, and no evidence of DNA fragmentation or significant chromatin condensation (53, 55). These characteristics are indicative of necrosis-like programmed cell death (46) where the pathways leading to rapid PS exposure and cell death still remain to be delineated.

The difference between the percentage of cell death observed in T cells upon CD44 cross-linking vs the addition of HA suggests that HA-induced death may be limited to cells that exhibit high levels of HA binding. In vitro, using purified HA, this appears to be ~10% of activated T cells; although this only became evident after blockage of Fas-mediated AICD. However, this percentage may be greater in vivo as HA binding proteins present in the extracellular matrix have been shown to enhance HA binding to CD44 (56, 57). Indeed, an in vivo role for CD44 in AICD has been suggested to explain the increased severity of Con A induced hepatitis (25) and the delayed-type hypersensitivity response (24) in $CD44^{-/-}$ mice.

CD44 mAbs that bind to the HA binding site of CD44 were efficient at inducing cell death in activated T cells, whereas Hermes-3, a mAb that binds to CD44 at another site, did not. This infers that a specific interaction with the HA binding site of CD44 is required to induce cell death. HA binding may facilitate a conformational change in CD44 or its repeating structure may facilitate clustering, which then transmits a signal to the cell. The response to HA may relate to the avidity of the interaction with CD44, as there was a correlation between the level of HA binding and cell death. A reduced ability of low molecular mass HA to engage multiple CD44 molecules or facilitate clustering may help explain its inability to enhance AICD in the transfected Jurkat cells. It is tempting to speculate that low molecular mass or fragmented HA in inflamed tissue could reduce CD44-dependent AICD, thereby maintaining T cell activation and promoting the inflammatory response, whereas newly synthesized high molecular mass HA, produced to facilitate tissue repair, could increase AICD and thus promote contraction of the immune response and restoration of immune homeostasis. However, it is currently unclear what effect the presence of cells undergoing necrotic-like programmed cell death would have on the inflammatory response. One possibility is that loss of membrane integrity occurs before phagocytosis and the release of cytoplasmic contents would result in immune cell activation similar to what is observed in the presence necrotic cells. Alternatively, as PS exposure is sufficient to target cells for recognition, phagocytosis, and subsequent degradation by macrophages (reviewed in Ref. 58); high HA binding by activated T cells may trigger PS exposure and flag these cells for rapid removal. High HA binding may be a characteristic of highly active T cells, as increased CD44 expression is a marker for activated T cells and HA binding identifies highly active T regulatory cells (59). Levels of CD44 expression and HA binding by T cells could therefore be important for the initiation of inflammation due to their role in extravasation, and be important for the resolution of inflammation due to their ability to mediate AICD in T cells.

Acknowledgments

We thank Andy Johnson at the University of British Columbia (Vancouver, British Columbia, Canada) Flow Cytometry Facility for cell sorting. We also thank Jennifer Cox, Chris Overall, and Nina Maeshima for providing MRL/*lpr* and C57BL/6 spleens, and N. Maeshima for comments on the manuscript.

Disclosures

The authors have no financial conflict of interest.

References

1. Ponta, H., L. Sherman, and P. A. Herrlich. 2003. CD44: from adhesion molecules to signalling regulators. *Nat. Rev. Mol. Cell Biol.* 4: 33–45.
2. Johnson, P., A. Maiti, K. L. Brown, and R. Li. 2000. A role for the cell adhesion molecule CD44 and sulfation in leukocyte-endothelial cell adhesion during an inflammatory response? *Biochem. Pharm.* 59: 455–465.
3. Pure, E., and C. A. Cuff. 2001. A crucial role for CD44 in inflammation. *Trends Mol. Med.* 7: 213–221.
4. Lesley, J., R. Hyman, N. English, J. B. Catterall, and G. A. Turner. 1997. CD44 in inflammation and metastasis. *Glycoconj. J.* 14: 611–622.
5. Stern, R., A. A. Asari, and K. N. Sugahara. 2006. Hyaluronan fragments: an information-rich system. *Eur. J. Cell Biol.* 85: 699–715.
6. Toole, B. P. 2004. Hyaluronan: from extracellular glue to pericellular cue. *Nat. Rev. Cancer* 4: 528–539.
7. Cuff, C. A., D. Kothapalli, I. Azonobi, S. Chun, Y. M. Zhang, R. Belkin, C. Yeh, A. Secreto, R. K. Assoian, D. J. Rader, and E. Pure. 2001. The adhesion receptor CD44 promotes atherosclerosis by mediating inflammatory cell recruitment and vascular cell activation. *J. Clin. Invest.* 108: 1031–1040.
8. Stoop, R., H. Kotani, J. D. McNeish, I. G. Otterness, and K. Mikecz. 2001. Increased resistance to collagen-induced arthritis in CD44-deficient DBA/1 mice. *Arthritis Rheum.* 44: 2922–2931.
9. Teder, P., R. W. Vandivier, D. Jiang, J. Liang, L. Cohn, E. Pure, P. M. Henson, and P. W. Noble. 2002. Resolution of lung inflammation by CD44. *Science* 296: 155–158.
10. Hayer, S., G. Steiner, B. Gortz, E. Reiter, M. Tohidast-Akrad, M. Amling, O. Hoffmann, K. Redlich, J. Zwerina, K. Skriner, et al. 2005. CD44 is a determinant of inflammatory bone loss. *J. Exp. Med.* 201: 903–914.
11. Budd, R. C., J. C. Cerottini, C. Horvath, C. Bron, T. Pedrazzini, R. C. Howe, and H. R. MacDonald. 1987. Distinction of virgin and memory T lymphocytes: stable acquisition of the Pgp-1 glycoprotein concomitant with antigenic stimulation. *J. Immunol.* 138: 3120–3129.

12. Lesley, J., N. Howes, A. Perschl, and R. Hyman. 1994. Hyaluronan binding function of CD44 is transiently activated on T cells during an in vivo immune response. *J. Exp. Med.* 180: 383–387.
13. Lesley, J., R. Hyman, and P. W. Kincade. 1993. CD44 and its interaction with extracellular matrix. *Adv. Immunol.* 54: 271–335.
14. Galandrini, R., E. Galluzzo, N. Albi, C. E. Grossi, and A. Velardi. 1994. Hyaluronate is costimulatory for human T cell effector functions and binds to CD44 on activated T cells. *J. Immunol.* 153: 21–31.
15. Mummert, M. E., D. Mummert, D. Edelbaum, F. Hui, H. Matsue, and A. Takashima. 2002. Synthesis and surface expression of hyaluronan by dendritic cells and its potential role in antigen presentation. *J. Immunol.* 169: 4322–4331.
16. Do, Y., P. S. Nagarkatti, and M. Nagarkatti. 2004. Role of CD44 and hyaluronic acid (HA) in activation of alloreactive and antigen-specific T cells by bone marrow-derived dendritic cells. *J. Immunother.* 27: 1–12.
17. Termeer, C., F. Benedix, J. Sleeman, C. Fieber, U. Voith, T. Ahrens, K. Miyake, M. Freudenberg, C. Galanos, and J. C. Simon. 2002. Oligosaccharides of hyaluronan activate dendritic cells via toll-like receptor 4. *J. Exp. Med.* 195: 99–111.
18. DeGrendele, H. C., P. Estess, L. J. Picker, and M. H. Siegelman. 1996. CD44 and its ligand hyaluronate mediate rolling under physiologic flow–a novel lymphocyte–endothelial cell primary adhesion pathway. *J. Exp. Med.* 183: 1119–1130.
19. Mohamadzadeh, M., H. Degrendele, H. Arizpe, P. Estess, and M. Siegelman. 1998. Proinflammatory stimuli regulate endothelial hyaluronan expression and CD44/HA-dependent primary adhesion. *J. Clin. Invest.* 101: 97–108.
20. Bonder, C. S., S. R. Clark, M. U. Norman, P. Johnson, and P. Kubes. 2006. Use of CD44 by $CD4^+$ Th1 and Th2 lymphocytes to roll and adhere. *Blood* 107: 4798–4806.
21. Nandi, A., P. Estess, and M. Siegelman. 2004. Bimolecular complex between rolling and firm adhesion receptors required for cell arrest; CD44 association with VLA-4 in T cell extravasation. *Immunity* 20: 455–465.
22. DeGrendele, H. C., P. Estess, and M. H. Siegelman. 1997. Requirement for CD44 in activated T cell extravasation into an inflammatory site. *Science* 278: 672–675.
23. Krammer, P. H., R. Arnold, and I. N. Lavrik. 2007. Life and death in peripheral T cells. *Nat. Rev. Immunol.* 7: 532–542.
24. McKallip, R. J., Y. Do, M. T. Fisher, J. L. Robertson, P. S. Nagarkatti, and M. Nagarkatti. 2002. Role of CD44 in activation-induced cell death: CD44-deficient mice exhibit enhanced T cell response to conventional and superantigens. *Int. Immunol.* 14: 1015–1026.
25. Chen, D., R. J. McKallip, A. Zeytun, Y. Do, C. Lombard, J. L. Robertson, T. W. Mak, P. S. Nagarkatti, and M. Nagarkatti. 2001. CD44-deficient mice exhibit enhanced hepatitis after concanavalin A injection: evidence for involvement of CD44 in activation-induced cell death. *J. Immunol.* 166: 5889–5897.
26. Do, Y., A. Q. Rafi-Janajreh, R. J. McKallip, P. S. Nagarkatti, and M. Nagarkatti. 2003. Combined deficiency in CD44 and Fas leads to exacerbation of lymphoproliferative and autoimmune disease. *Int. Immunol.* 15: 1327–1340.
27. Weber, G. F. 2004. The absence of CD44 ameliorates Fas(lpr/lpr) disease. *Autoimmunity* 37: 1–8.
28. Mielgo, A., V. Brondani, L. Landmann, A. Glaser-Ruhm, P. Erb, D. Stupack, and U. Gunthert. 2007. The CD44 standard/ezrin complex regulates Fas-mediated apoptosis in Jurkat cells. *Apoptosis* 12: 2051–2061.
29. Nakano, K., K. Saito, S. Mine, S. Matsushita, and Y. Tanaka. 2007. Engagement of CD44 up-regulates Fas ligand expression on T cells leading to activation-induced cell death. *Apoptosis* 12: 45–54.
30. Ayroldi, E., L. Cannarile, G. Migliorati, A. Bartoli, I. Nicoletti, and C. Riccardi. 1995. CD44 (Pgp-1) inhibits CD3 and dexamethasone-induced apoptosis. *Blood* 86: 2672–2678.
31. Larkin, J., G. J. Renukaradhya, V. Sriram, W. Du, J. Gervay-Hague, and R. R. Brutkiewicz. 2006. CD44 differentially activates mouse NK T cells and conventional T cells. *J. Immunol.* 177: 268–279.
32. Dougherty, G. J., D. L. Cooper, J. F. Memory, and R. K. Chiu. 1994. Ligand binding specificity of alternatively spliced CD44 isoforms: recognition and binding of hyaluronan by CD44R1. *J. Biol. Chem.* 269: 9074–9078.
33. de Belder, A. N., and K. O. Wik. 1975. Preparation and properties of fluorescein-labelled hyaluronate. *Carbohydr. Res.* 44: 251–257.
34. Dougherty, G. J., P. M. Lansdorp, D. L. Cooper, and R. K. Humphries. 1991. Molecular cloning of CD44R1 and CD44R2, two novel isoforms of the human CD44 lymphocyte "homing" receptor expressed by hemopoetic cells. *J. Exp. Med.* 174: 1–5.
35. Ruffell, B., and P. Johnson. 2005. Chondroitin sulfate addition to CD44H negatively regulates hyaluronan binding. *Biochem. Biophys. Res. Commun.* 334: 306–312.
36. Ikegami-Kawai, M., and T. Takahashi. 2002. Microanalysis of hyaluronan oligosaccharides by polyacrylamide gel electrophoresis and its application to assay of hyaluronidase activity. *Anal. Biochem.* 311: 157–165.
37. Schmits, R., J. Filmus, N. Gerwin, G. Senaldi, F. Kiefer, T. Kundig, A. Wakeham, A. Shahinian, C. Catzavelos, J. Rak, et al. 1997. CD44 regulates hematopoietic progenitor distribution, granuloma formation and tumorigenicity. *Blood* 90: 2217–2233.
38. Peach, R. J., D. Hollenbaugh, I. Stamenkovic, and A. Aruffo. 1993. Identification of hyaluronic acid binding sites in the extracellular domain of CD44. *J. Cell Biol.* 122: 257–264.
39. Bajorath, J., B. Greenfield, S. B. Munro, A. J. Day, and A. Aruffo. 1998. Identification of CD44 residues important for hyaluronan binding and delineation of the binding site. *J. Biol. Chem.* 273: 338–343.
40. Holmstrom, T. H., S. C. Chow, I. Elo, E. T. Coffey, S. Orrenius, L. Sistonen, and J. E. Eriksson. 1998. Suppression of Fas/APO-1-mediated apoptosis by mitogen-activated kinase signaling. *J. Immunol.* 160: 2626–2636.
41. Makatsori, E., N. K. Karamanos, N. Papadogiannakis, A. Hjerpe, E. D. Anastassiou, and T. Tsegenidis. 2001. Synthesis and distribution of glycosaminoglycans in human leukemic B- and T-cells and monocytes studied using specific enzymic treatments and high-performance liquid chromatography. *Biomed. Chromatogr.* 15: 413–417.
42. Ayroldi, E., L. Cannarile, and C. Riccardi. 1996. Modulation of superantigen-induced t-cell deletion by antibody anti-pgp-1 (cd44). *Immunology* 87: 191–197.
43. Latinis, K. M., L. L. Carr, E. J. Peterson, L. A. Norian, S. L. Eliason, and G. A. Koretzky. 1997. Regulation of CD95 (Fas) ligand expression by TCR-mediated signaling events. *J. Immunol.* 158: 4602–4611.
44. Hildeman, D. A., T. Mitchell, T. K. Teague, P. Henson, B. J. Day, J. Kappler, and P. C. Marrack. 1999. Reactive oxygen species regulate activation-induced T cell apoptosis. *Immunity* 10: 735–744.
45. Scaffidi, C., S. Fulda, A. Srinivasan, C. Friesen, F. Li, K. J. Tomaselli, K. M. Debatin, P. H. Krammer, and M. E. Peter. 1998. Two CD95 (APO-1/Fas) signaling pathways. *EMBO J.* 17: 1675–1687.
46. Jaattela, M., and J. Tschopp. 2003. Caspase-independent cell death in T lymphocytes. *Nat. Immunol.* 4: 416–423.
47. Frankfurt, O. S., and A. Krishan. 2001. Identification of apoptotic cells by formamide-induced DNA denaturation in condensed chromatin. *J. Histochem. Cytochem.* 49: 369–378.
48. Lenardo, M. J. 1991. Interleukin-2 programs mouse $\alpha\ \beta$ T lymphocytes for apoptosis. *Nature* 353: 858–861.
49. Artus, C., E. Maquarre, R. S. Moubarak, C. Delettre, C. Jasmin, S. A. Susin, and J. Robert-Lezenes. 2006. CD44 ligation induces caspase-independent cell death via a novel calpain/AIF pathway in human erythroleukemia cells. *Oncogene* 25: 5741–5751.
50. Ly, J. D., D. R. Grubb, and A. Lawen. 2003. The mitochondrial membrane potential (δpsi(m)) in apoptosis; an update. *Apoptosis* 8: 115–128.
51. Deas, O., C. Dumont, M. MacFarlane, M. Rouleau, C. Hebib, F. Harper, F. Hirsch, B. Charpentier, G. M. Cohen, and A. Senik. 1998. Caspase-independent cell death induced by anti-CD2 or staurosporine in activated human peripheral T lymphocytes. *J. Immunol.* 161: 3375–3383.
52. Klaus, S. J., S. P. Sidorenko, and E. A. Clark. 1996. CD45 ligation induces programmed cell death in T and B lymphocytes. *J. Immunol.* 156: 2743–2753.
53. Mateo, V., L. Lagneaux, D. Bron, G. Biron, M. Armant, G. Delespesse, and M. Sarfati. 1999. CD47 ligation induces caspase-independent cell death in chronic lymphocytic leukemia. *Nat. Med.* 5: 1277–1284.
54. Pettersen, R. D., G. Bernard, M. K. Olafsen, M. Pourtein, and S. O. Lie. 2001. CD99 signals caspase-independent T cell death. *J. Immunol.* 166: 4931–4942.
55. Lesage, S., A. M. Steff, F. Philippoussis, M. Page, S. Trop, V. Mateo, and P. Hugo. 1997. CD4+ CD8+ thymocytes are preferentially induced to die following CD45 cross-linking, through a novel apoptotic pathway. *J. Immunol.* 159: 4762–4771.
56. Lesley, J., I. Gal, D. J. Mahoney, M. R. Cordell, M. S. Rugg, R. Hyman, A. J. Day, and K. Mikecz. 2004. TSG-6 modulates the interaction between hyaluronan and cell surface CD44. *J. Biol. Chem.* 279: 25745–25754.
57. Zhuo, L., A. Kanamori, R. Kannagi, N. Itano, J. Wu, M. Hamaguchi, N. Ishiguro, and K. Kimata. 2006. SHAP potentiates the CD44-mediated leukocyte adhesion to the hyaluronan substratum. *J. Biol. Chem.* 281: 20303–20314.
58. Schlegel, R. A., M. K. Callahan, and P. Williamson. 2000. The central role of phosphatidylserine in the phagocytosis of apoptotic thymocytes. *Ann. NY Acad. Sci.* 926: 217–225.
59. Firan, M., S. Dhillon, P. Estess, and M. H. Siegelman. 2006. Suppressor activity and potency among regulatory T cells is discriminated by functionally active CD44. *Blood* 107: 619–627.